Supporting Information for:

Large Grounds-State Entropy Changes for Hydrogen Atom Transfer Reactions of Iron Complexes

*Elizabeth A. Mader, Ernest R. Davidson, and James M. Mayer**

University of Washington, Department of Chemistry,

Box 351700, Seattle, WA, 98195-1700.

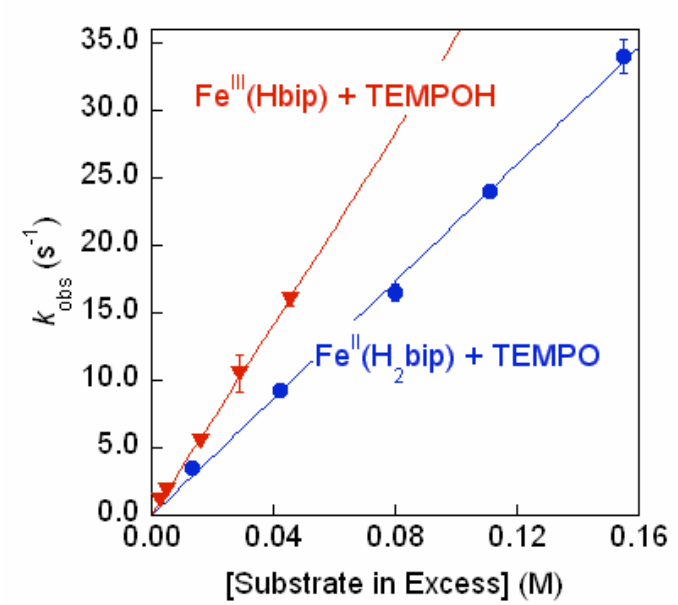

Figure S1. Plot of the observed pseudo-first order rate constants for 0.1 mM **$Fe^{II}(H_2bip)$** + excess TEMPO (blue ●) and 0.1 mM **Fe^{III}(Hbip)** + excess TEMPOH (red ▼) in MeCN at T= 46ºC.

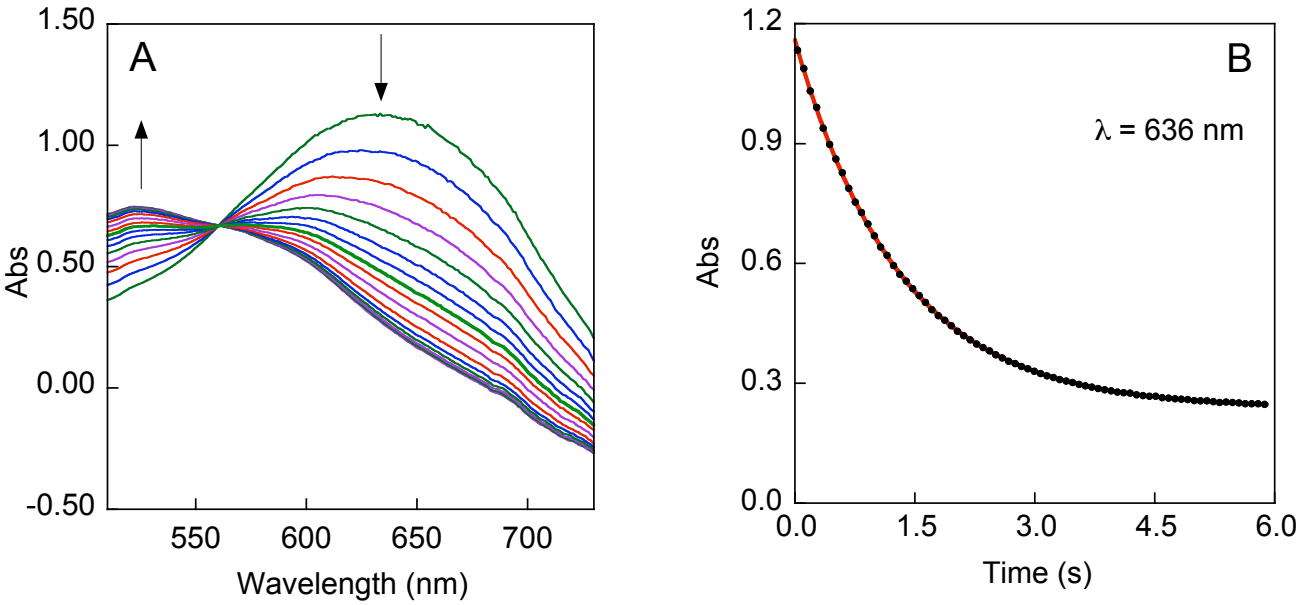

Figure S2. A) Evolution of the of the UV-Visible spectrum of 0.4 mM **Fe^{III}(Hbip)** in the presence of 3.9mM TEMPOH (eq 5) over the course of 6 s at T = 25 ºC in MeCN. B) Match between the original data (•) and the pseudo first order fit (–) resulting from Olis SVD Global Analysis[1] with over the whole wavelength region in **A**. Shown only for a single wavelength, 636 nm.

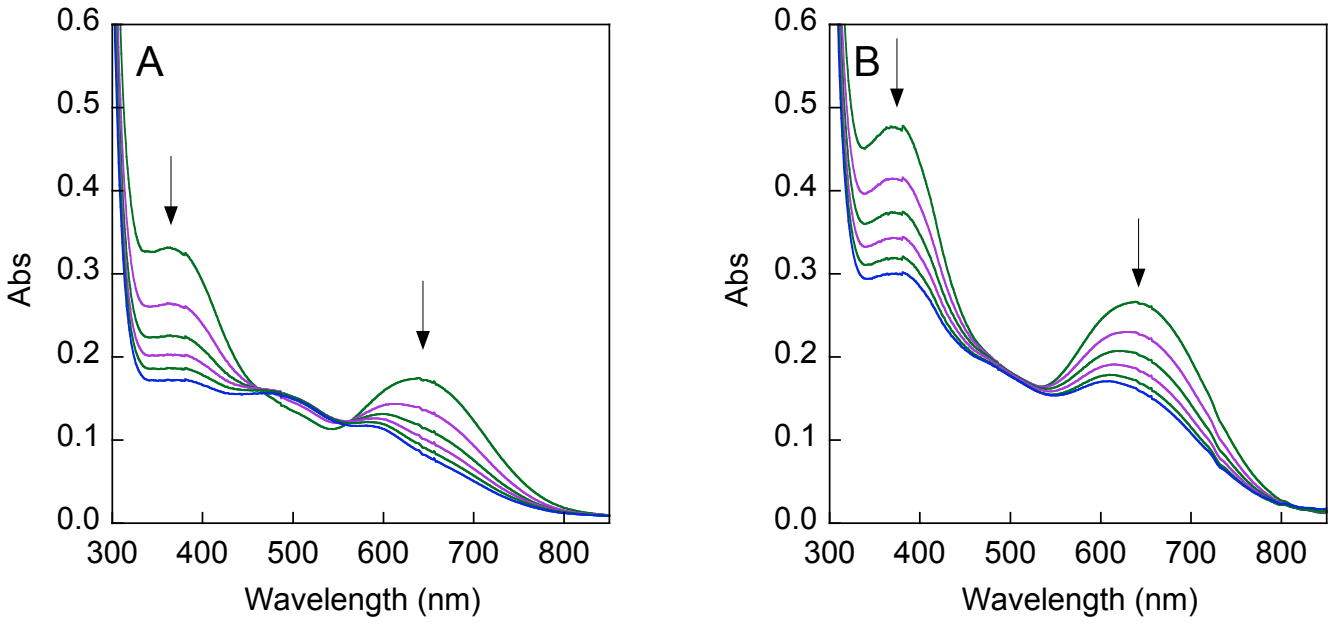

Figure S3. Measurement of K_5 by static UV-visible spectrophotometry at 298 K. (**A**) Addition of 5 × 100 µL increments of 0.13 M TEMPO-H (65 µmol total) to a mixture of 0.154 µmol **$Fe^{III}(H_2bip)$** and 19.4 µmol TEMPO in 2.350 mL MeCN. (B) Addition of 5 × 100 µL increments of 0.15 M TEMPO-H (73 µM total) to a mixture of 0.127 µmol **$Fe^{III}(H_2bip)$** and 17.3 µmol TEMPO in 2.100 mL CH_2Cl_2.

Table S1: Equilibrium constants as independently determined from each spectrum in Figure S3.

Spectrum	K_5 MeCN	K_5 CH_2Cl_2
1	1.85	3.70
2	1.85	3.84
3	1.82	4.00
4	1.82	4.17
5	1.82	4.35
Average ± Std. Dev.	1.82 ± 0.03	4.0 ± 0.3

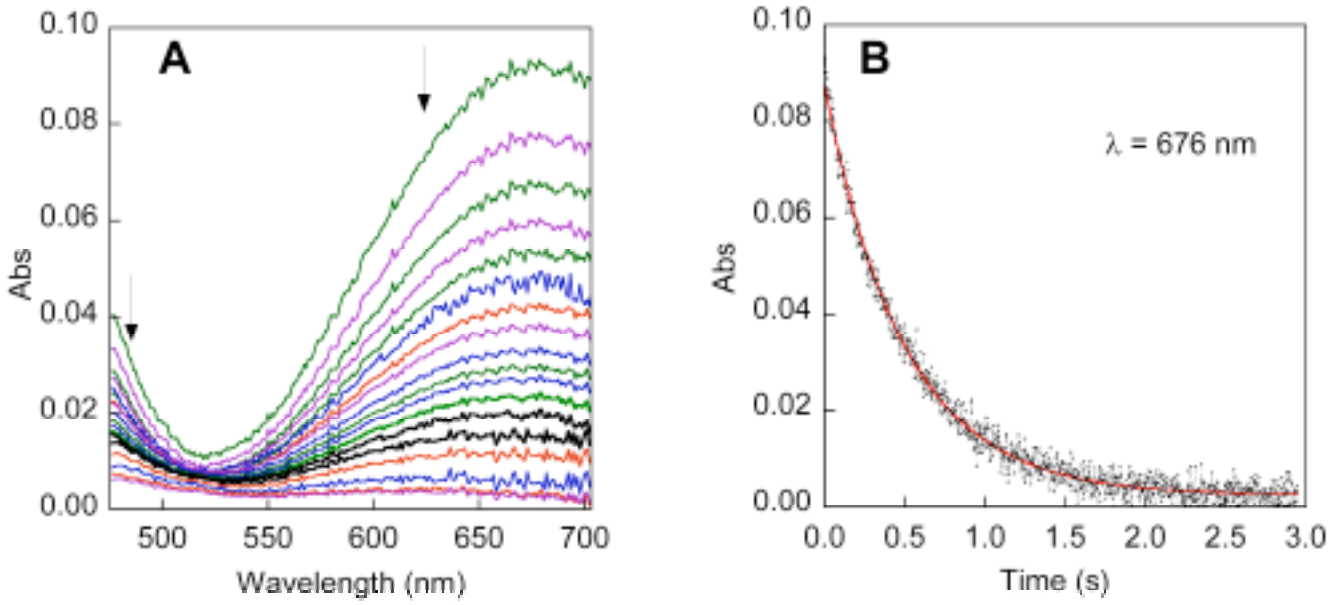

Figure S4. A) Evolution of the of the UV-Visible spectrum of 2.1×10^{-5} M **Fe^{III}(Hbim)** in the presence of 0.65 mM TEMPOH (eq 6) over the course of 3 s at T = 25 ºC in MeCN. B) Match between the original data (•) and the pseudo first order fit (–) resulting from Olis SVD Global Analysis[1] with over the whole wavelength region in **A**. Shown only for a single wavelength, 676 nm.

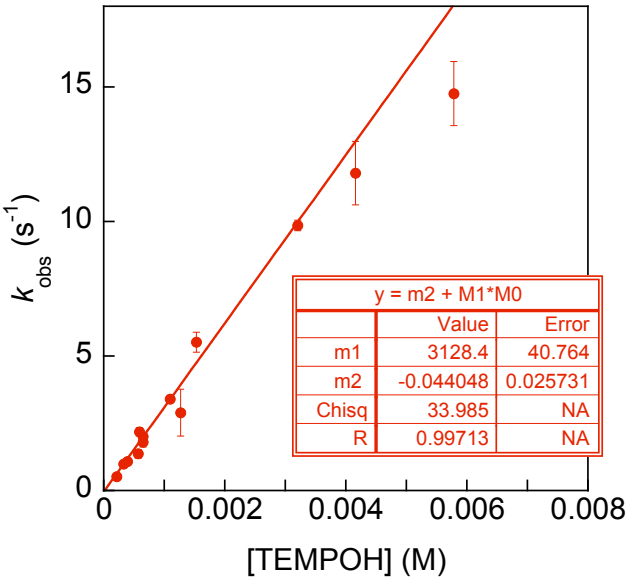

Figure S5. Plot of the observed pseudo-first order rate constants for 2.1×10^{-5} M **Fe^{III}(Hbim)** + excess TEMPO-H in MeCN at T= 25ºC.

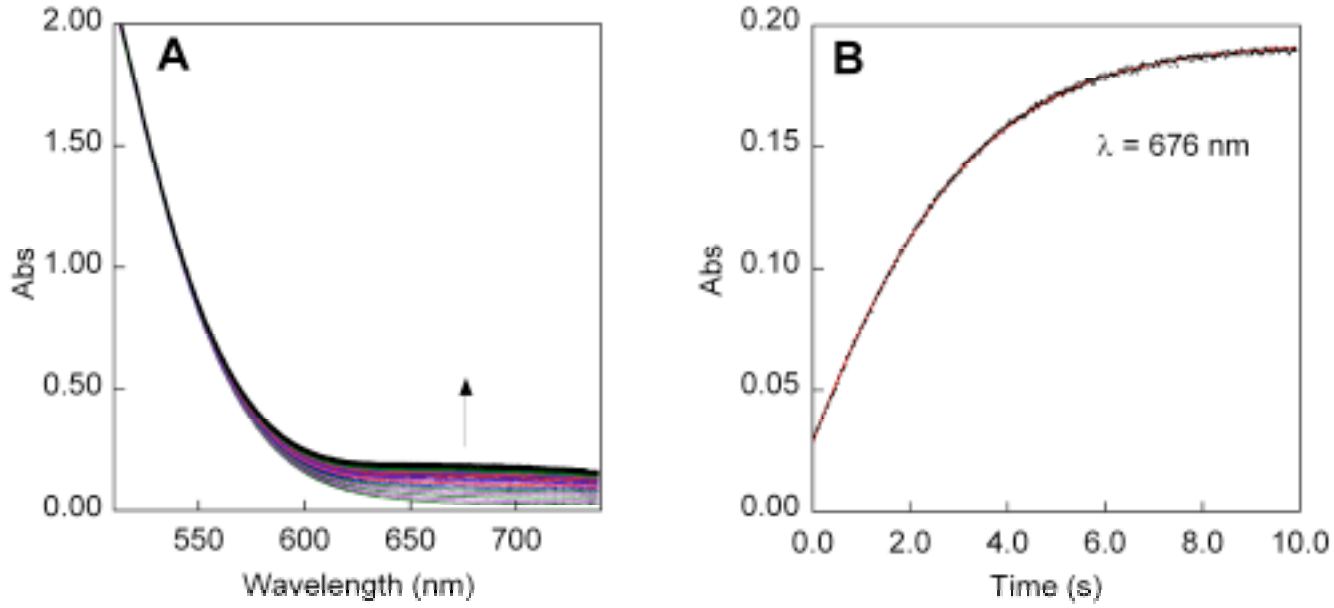

Figure S6. A) Evolution of the of the UV-Visible spectrum of 0.09 mM **$Fe^{II}(H_2bim)$** in the presence of 0.28 M TEMPO (eq 6) over the course of 10 s at T = 25 ºC in MeCN. B) Match between the original data (•) and the approach to equilibrium second order fit (–) resulting from SVD global analysis with Specfit[2] over the whole wavelength region in **A**. Shown only for a single wavelength, 676 nm.

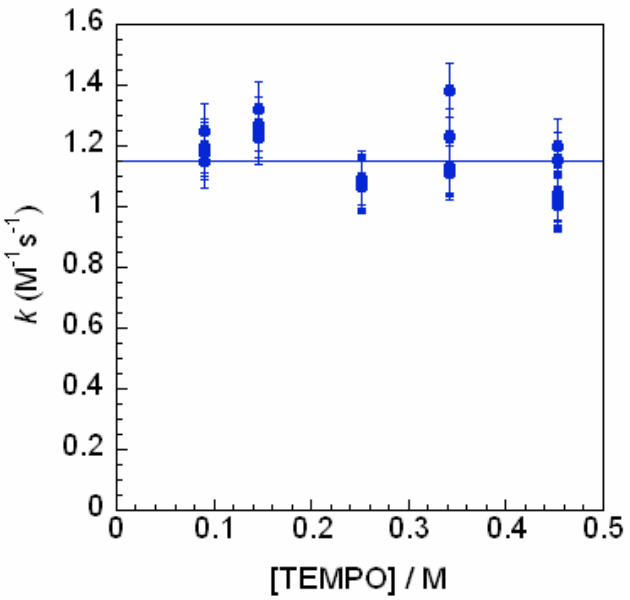

Figure S7. Plot of the second-order rate constants (k_6) for 0.07 mM **$Fe^{II}(H_2bim)$** with varying TEMPO concentrations directly obtained from Specfit.[2] T= 44 ºC in MeCN.

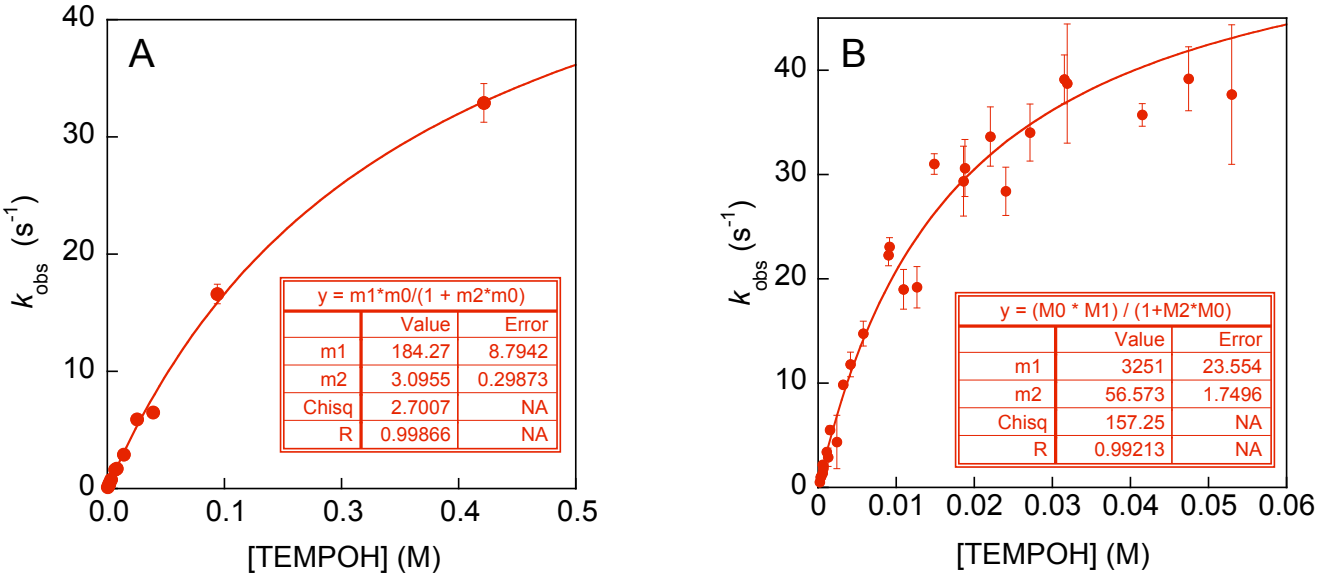

Figure S8. Saturation kinetics plot for (A) **Fe^{III}(Hbip)** + TEMPO-H and (B) **Fe^{III}(Hbim)** + TEMPOH fit to eq 9 in MeCN at 298 K. For **Fe^{III}(Hbip)** + TEMPO-H: K_{8A} = m2 = 3.1 ± 0.3 M^{-1}, k_{8B} = m1/m2 = 59 ± 6 $M^{-1}s^{-1}$. For **Fe^{III}(Hbim)** + TEMPO-H: K_{8A} = m2 = 56.6 ± 1.7 M^{-1}, k_{8B} = m1/m2 = 57.4 ± 1.8 $M^{-1}s^{-1}$.

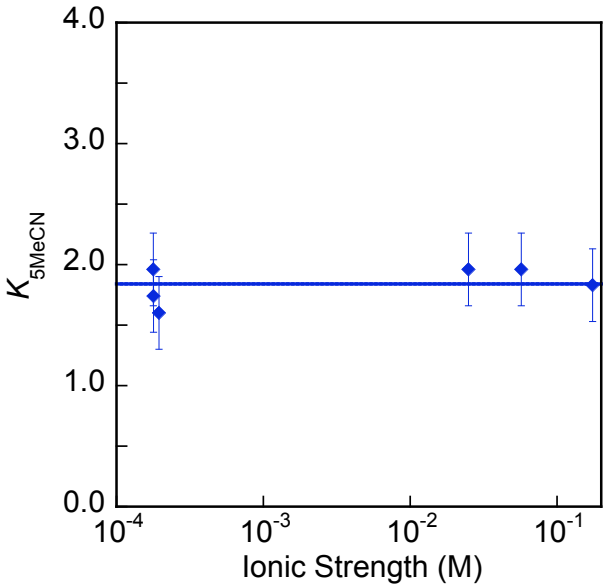

Figure S9: Dependence of K_5 on added $(Bu)_4NClO_4$ in MeCN at 298 K.

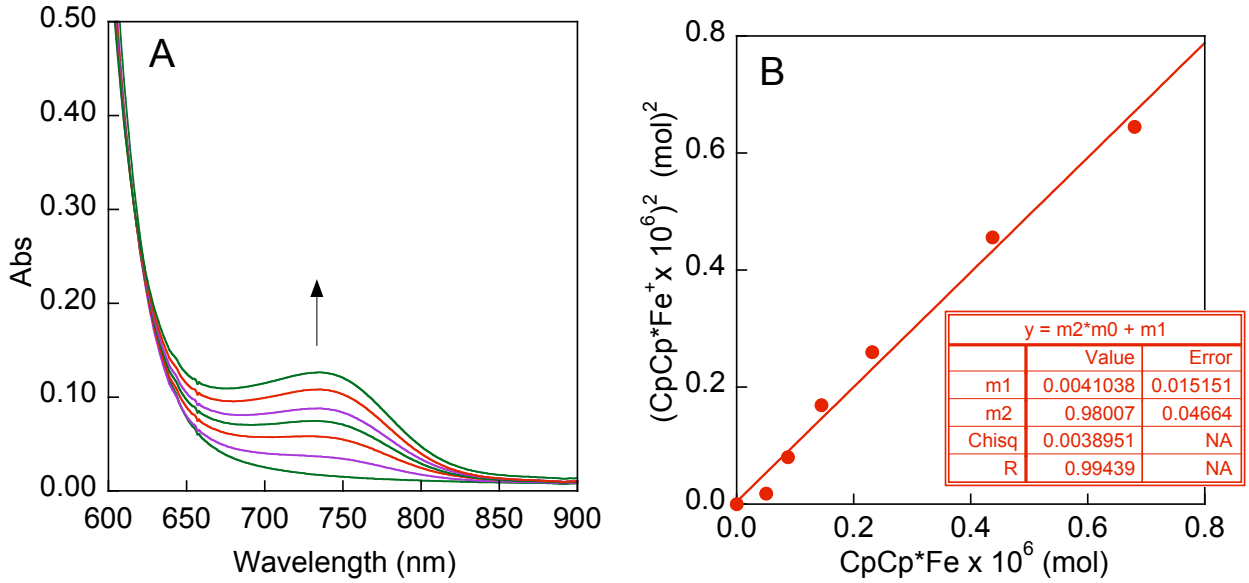

Figure S10. Measurement of $\mathbf{Fe^{II}(H_2bim)}$ + $[CpCp^*Fe]^+$ ⇆ $\mathbf{Fe^{III}(H_2bim)}$ + $CpCp^*Fe$; K_{10} - in MeCN at 298 K. (**A**) UV-visible spectra of 4.7 µmol $\mathbf{Fe^{III}(H_2bim)}$ upon the addition of 6 × 0.18 µmol increments of $CpCp^*Fe$ (0-1.5 µmol total) in 0.09M $^n Bu_4NClO_4$. (**B**) Determination of K_{10}. Plot of (mol $CpCp^*Fe)^2$ vs mol $CpCp^*Fe$ should be linear with slope = m2 = $\mathbf{Fe^{III}(H_2bim)}$ / K_{10}**.** For this sample K_{10} = 4.8 ± 0.1 using absorbance data at 740 nm.

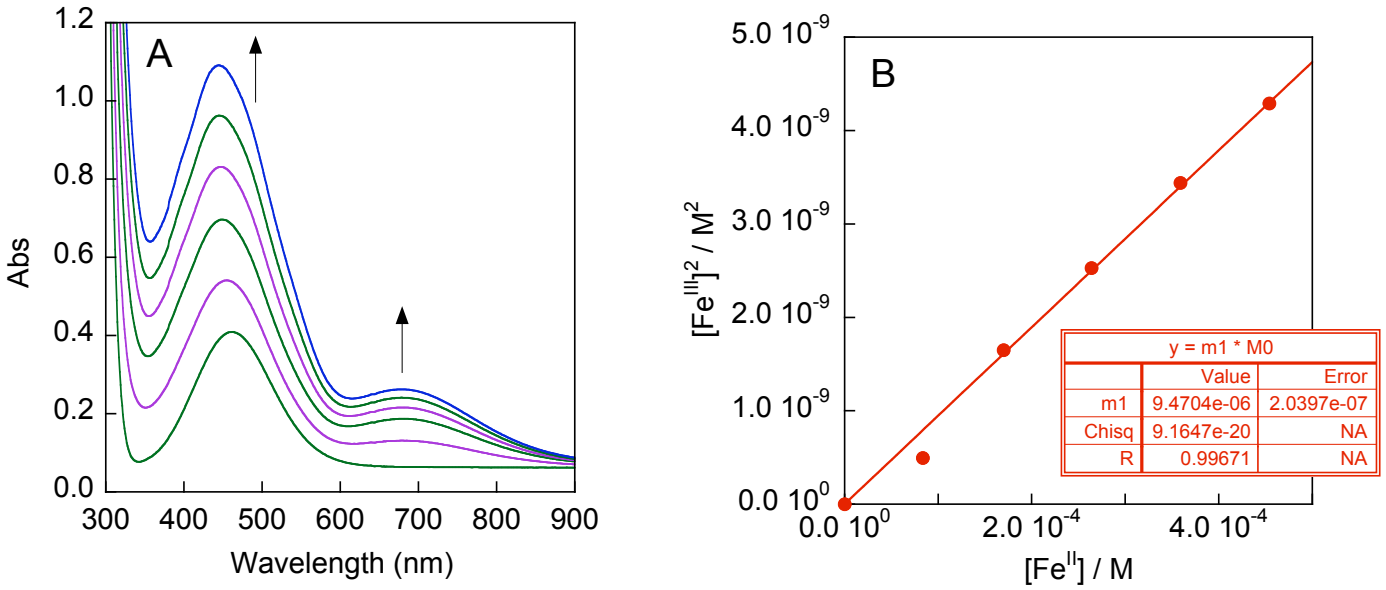

Figure S11. Measurement of K_6 by static UV-visible spectrophotometry at 298 K in MeCN. (**A**) Addition of 5 × 10 µL increments of 21.3 mM **$Fe^{II}(H_2bim)$** (52 µM total) to 64.6 µmol TEMPO in 2.00 mL MeCN. (B) Plot of $[Fe^{III}]^2$ vs $[Fe^{II}]$ using absorbance data at 676 nm. Plot should be linear with slope = m1 = K_6 × [TEMPO]. For this sample K_6 = 3300 ± 100.

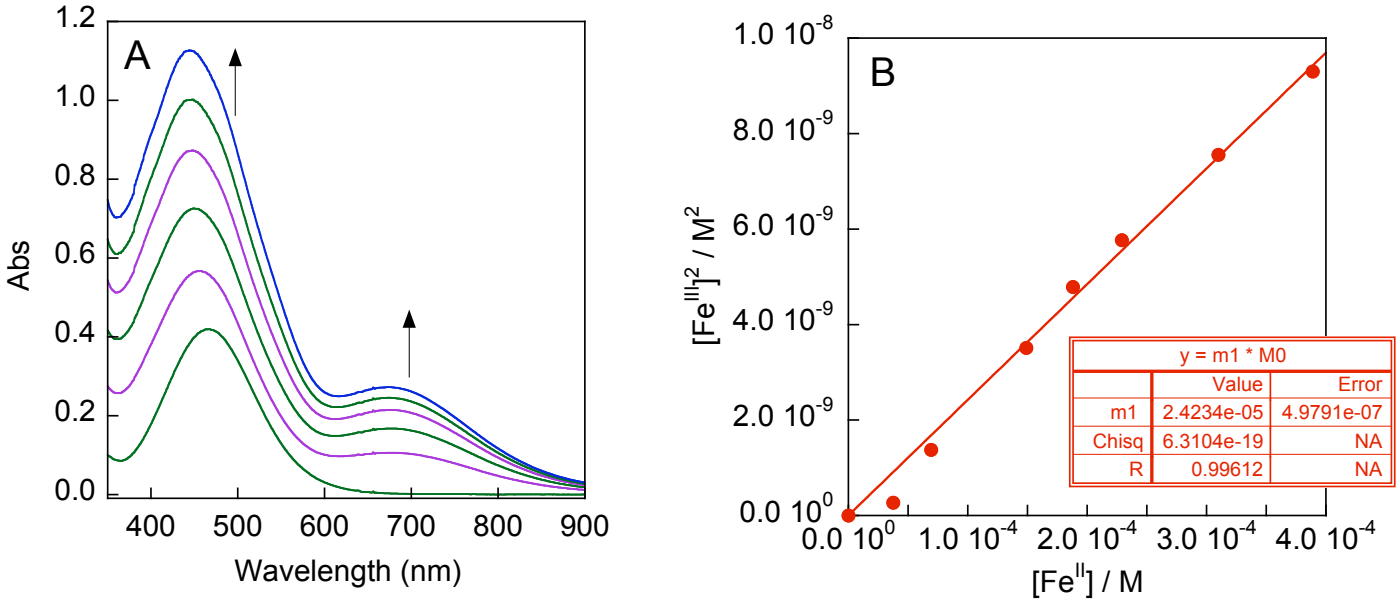

Figure S12. Measurement of K_6 by static UV-visible spectrophotometry at 298 K in acetone. (**A**) Addition of 5 × 50 µL increments of 19.4 mM **$Fe^{II}(H_2bim)$** (48.5 µM total) to 77.1 µmol TEMPO in 2.00 mL acetone. (B) Plot of $[Fe^{III}]^2$ vs $[Fe^{II}]$ using absorbance data at 676 nm. Plot should be linear with slope = m1 = K_6*[TEMPO]. For this sample K_6 = 1540 ± 50.

Table S2. Energies, molar heat capacities, and entropies for vibrational modes in the product of Eq 12.

	E (kcal mol^{-1})	C_V (cal mol^{-1} K^{-1})	S (cal mol^{-1} K^{-1}).
TOTAL	243.209	78.797	166.131
ELECTRONIC	0	0	3.561
TRANSLATIONAL	0.889	2.981	43.350
ROTATIONAL	0.889	2.981	34.420
VIBRATIONAL	241.432	72.836	84.801
VIBRATION 1	0.593	1.985	6.284
VIBRATION 2	0.594	1.982	5.341
VIBRATION 3	0.596	1.977	4.736
VIBRATION 4	0.597	1.972	4.380
VIBRATION 5	0.598	1.969	4.169
VIBRATION 6	0.599	1.965	3.978
VIBRATION 7	0.599	1.964	3.944
VIBRATION 8	0.601	1.958	3.720
VIBRATION 9	0.603	1.952	3.519
VIBRATION 10	0.604	1.948	3.418
VIBRATION 11	0.606	1.942	3.289
VIBRATION 12	0.611	1.926	2.994
VIBRATION 13	0.615	1.912	2.787
VIBRATION 14	0.630	1.866	2.320
VIBRATION 15	0.638	1.838	2.121
VIBRATION 16	0.647	1.813	1.969
VIBRATION 17	0.647	1.812	1.964
VIBRATION 18	0.653	1.793	1.868
VIBRATION 19	0.657	1.780	1.809
VIBRATION 20	0.662	1.766	1.743
VIBRATION 21	0.664	1.760	1.717
VIBRATION 22	0.679	1.712	1.540
VIBRATION 23	0.701	1.650	1.351
VIBRATION 24	0.703	1.644	1.334
VIBRATION 25	0.711	1.620	1.270
VIBRATION 26	0.720	1.596	1.214
VIBRATION 27	0.721	1.593	1.206
VIBRATION 28	0.734	1.556	1.125
VIBRATION 29	0.749	1.514	1.041
VIBRATION 30	0.824	1.325	0.748
VIBRATION 31	0.871	1.215	0.619
VIBRATION 32	0.882	1.191	0.594
VIBRATION 33	0.891	1.170	0.574
VIBRATION 34	0.931	1.086	0.496

Table S3. Energies, molar heat capacities, and entropies for vibrational modes in the reactant of Eq 12.

	E (kcal mol^{-1})	C_V (cal mol^{-1} K^{-1})	S (cal mol^{-1} K^{-1}).
TOTAL	241.633	83.231	184.814
ELECTRONIC	0	0	3.561
TRANSLATIONAL	0.889	2.981	43.350
ROTATIONAL	0.889	2.981	34.676
VIBRATIONAL	239.856	77.269	103.229
VIBRATION 1	0.593	1.986	6.898
VIBRATION 2	0.594	1.984	5.843
VIBRATION 3	0.594	1.981	5.258
VIBRATION 4	0.595	1.980	5.051
VIBRATION 5	0.595	1.978	4.828
VIBRATION 6	0.596	1.976	4.688
VIBRATION 7	0.596	1.974	4.519
VIBRATION 8	0.597	1.972	4.336
VIBRATION 9	0.597	1.971	4.269
VIBRATION 10	0.599	1.967	4.063
VIBRATION 11	0.601	1.958	3.726
VIBRATION 12	0.602	1.957	3.680
VIBRATION 13	0.608	1.937	3.188
VIBRATION 14	0.608	1.935	3.153
VIBRATION 15	0.612	1.921	2.918
VIBRATION 16	0.616	1.909	2.744
VIBRATION 17	0.621	1.893	2.566
VIBRATION 18	0.624	1.883	2.467
VIBRATION 19	0.626	1.878	2.420
VIBRATION 20	0.627	1.874	2.390
VIBRATION 21	0.636	1.844	2.162
VIBRATION 22	0.643	1.824	2.035
VIBRATION 23	0.652	1.794	1.874
VIBRATION 24	0.656	1.782	1.816
VIBRATION 25	0.665	1.756	1.701
VIBRATION 26	0.668	1.747	1.666
VIBRATION 27	0.676	1.724	1.579
VIBRATION 28	0.676	1.721	1.571
VIBRATION 29	0.690	1.682	1.443
VIBRATION 30	0.789	1.410	0.867
VIBRATION 31	0.815	1.345	0.775
VIBRATION 32	0.828	1.314	0.735
VIBRATION 33	0.839	1.289	0.704
VIBRATION 34	0.851	1.261	0.670
VIBRATION 35	0.868	1.221	0.626
VIBRATION 36	0.940	1.068	0.480

Table S4: Temperature dependence of relevant extinction coefficients over 270-330 K.[a]

Species	λ (nm)	Solvent		
		MeCN	CH_2Cl_2	Acetone
$Fe^{II}(H_2bip)$	460	ε = (-5.4 ± 1.0)T + (3395 ± 303)	ε = 1440 ± 80	--
	510	ε = (-16.7 ± 1.9)T + (7201 ± 580)	ε = (14 ± 8)T + (6284 ± 2567)	--
	645	ε = (-4.25 ± 0.55)T + (2161 ± 168)	ε = 580 ± 30	--
Fe^{III}(Hbip)	460	ε = (4.0 ± 1.1)T + (73 ± 324)	ε = (-16.9 ± 10.7)T + (6821 ± 3375)	--
	510	ε = (3.1 ± 1.0)T + (224 ± 309)	ε = (-14 ± 7)T + (5734 ± 2314)	--
	645	ε = (-6.41 ± 0.58)T + (4863 ± 175)	ε = (-34 ± 13)T + (13048 ± 4199)	--
Fe^{III}(Hbim)	460	ε = 3170 ± 100	--	ε = 3600 ± 150
	472	ε = 2650 ± 80	--	ε = 3100 ± 100
	676	ε = 2900 ± 120	--	ε = 2700 ± 140
$Fe^{II}(H_2bim)$	460	ε = (-0.24 ± 0.90)T + (1023 ± 274)	--	ε = (-4.15 ± 1.38)T + (2302 ± 424)
	472	ε = (-1.41 ± 0.53)T + (1360 ± 163)	--	ε = (-4.3 ± 1.4)T + (2334 ± 430)
	676	ε = 40 ± 5	--	ε = 40 ± 10
TEMPO	460	ε = (-0.0253 ± 0.0009)T + (17.9 ± 0.3)	ε = 11.8 ± 0.1	ε = (-0.022 ± 0.002)T + (17.1 ± 0.6)
	472	ε = (-0.2371 ± 0.0009)T + (17.2 ± 0.3)	--	ε = (-0.0206 ± 0.0017)T + (16.8 ± 0.5)
	510	ε = (-0.0104 ± 0.0008)T + (9.7 ± 0.2)	ε = 7.2 ± 0.1	--
	645	ε = (4.9 ± 0.3)×10^{-5}T - (0.670 ± 0.009)	ε = 0.04 ± 0.05	--
	676	ε = 0.05 ± 0.05	--	ε = 0.05 ± 0.05
$[CpCp^*Fe]^+$	740	ε = (-0.94 ± 0.04)T + (633 ± 13)	--	--

[a] ε = extinction coefficient, $M^{-1}cm^{-1}$. T = Temperature, K. Equations apply over 270-330 K.

Crystal Structures. Crystals of **$Fe^{III}(H_2bip)$**•MeCN•Et_2O were obtained by slow diffusion of Et_2O into MeCN at room temperature. They were mounted on a cyroloop with Paratone® oil, and data was collected in a nitrogen gas stream at 100 K. Intensity data was collected on an Bruker Platform Apex CCD diffractometer. The data was integrated using the Bruker SAINT software program and scaled using Bruker SADABS software. Solution by direct methods (SIR-2004) produced a complete heavy atom phasing model consistent with the proposed structure. All non-hydrogen atoms were refined anisotropically by full-matrix least-squares (SHELXL-97). All hydrogen atoms were placed using a riding model and their positions constrained relative to their parent atom using the appropriate HFIX command in SHELXL-97. One molecule of acetonitrile and diethyl ether co-crystallized with the target complex. However, degradation of the crystal was quick, even under oil, with the diethyl ether apparently desolvating from the crystal. From the data collection, it is estimated that 80% of the Et_2O remained in the crystal, with about 20% desolvated and leaving an empty void as refined from the data collected.

Crystals of TEMPO-H•$^1/_3H_2O$ formed upon leaving sublimed TEMPO-H under static vacuum for two weeks at room temperature. They were mounted on a glass capillary with oil. Data was collected at 130 K on an Enraf-Nonius KappaCCD diffractometer equipped with a fine focus Mo-target X-ray tube. The data were integrated and scaled using hkl-2000. This program applies a multiplicative correction factor (S) to the observed intensities (I): $S = (e^{-2B(\sin^2\theta/\lambda^2)}) /$ scale. S is calculated from the scale and the B factor, which is determined for each frame and is then applied to I to give the corrected intensity (I_{corr}). Solution by direct methods (SIR-97) produced a complete heavy atom phasing model consistent with the proposed structure. All hydroxyl and water hydrogen atoms were located from the difference map and refined isotropically. The remainder of the hydrogen atoms were placed using a riding model. All non-hydrogen atoms were refined anisotropically by full-matrix least-squares (SHELX-97).

Table S5. Refinement data for TEMPO-H and $Fe^{III}(H_2bip)_3(ClO_4)$ crystal structures.

	3 TEMPO–H•H_2O	**$Fe^{III}(H_2bip)_3(ClO_4)_3$•MeCN•$Et_2O$**
Empirical formula	$C_{27}H_{59}N_3O_4$	$C_{30}H_{55}Cl_3FeN_{13}O_{13}$
Formula Weight	489.77	968.04
Temperature (K)	130(2)	100(2)
Wavelength (Å)	0.71073 A	0.71073
Crystal description / color	prism / colorless	block / red
Crystal system, space group	Triclinic, P-1 (No. 2)	Monoclinic, P2(1)/n
Unit cell dimensions (Å, deg)	a = 8.1380(4)	a = 9.906(3)
	b = 12.3840(8)	b = 21.996(7)
	c = 16.0280(10)	c = 19.615(6)
	α = 75.343(2)°	α = 90°
	β = 78.788(2)°	β = 104.005(4)°
	γ = 78.105(3)°	γ = 90°
Volume ($Å^3$)	1511.82(15)	4147(2)
Z, density (Mg/m^3)	2, 1.076	4, 1.366
μ (mm^{-1})	0.071	0.622
F(000)	548	1772
Crystal size (mm)	0.48 × 0.24 × 0.24	0.15 × 0.15 × 0.15
θ range for data collection (deg)	3.34° to 28.27°	2.13° to 25.03°
Index ranges	-10 ≤ h ≤ 10	-11 ≤ h ≤ 11
	-13 ≤ k ≤ 16	-26 ≤ k ≤ 26
	-17 ≤ l ≤ 21	-23 ≤ l ≤ 23
Reflections collected / unique	8656 / 6206	29784 / 7322
Completeness to θ	82.6%	99.9 %
Absorption correction	HKL-2000	Semi-empirical from equivalents
Max. and min. transmission	0.9832 and 0.9668	0.9124 and 0.9124
Refinement method	Full-matrix least-squares on F^2	Full-matrix least-squares on F^2
Data / restraints / parameters	6206 / 0 / 336	7322 / 0 / 545
R(int)	0.0649	0.0566
Goodness-of-fit on F^2	1.000	1.120
Final R, Rw ($I > 2\sigma I$)[a]	0.0633, 0.1407	0.0687, 0.1656
Largest diff. peak and hole ($e Å^{-3}$)	0.228 and -0.228	0.797 and -0.568

[a] $w = 1/[s^2(F_o^2) + (0.0450P)^2 + 0.0000P]$ where $P = (F_o^2 + 2F_c^2)/3$

Calculation of $\Delta S°[H^{\bullet}]$ in various solvents:

Table S6: Relevant parameters for calculation of $\Delta S°[H^{\bullet}]$ in various solvents.

Solvent	$S°_f[H^{\bullet}]_g$ [a]	$\Delta S°_{solvation}[H^{\bullet}]$ [b]	$T\Delta S°[H^{\bullet}]$ [c]
MeCN	27.419	-11.92 [d]	4.62
DMSO	27.419	-12.0 [e]	4.60
toluene	27.419	-11.40 [d]	4.78
1,2-dichloroethane	27.419	-11.1 [e]	4.87
DMF	27.419	-12.14 [d]	4.56
H_2O	27.419	-17.50[e,f]	2.96

[a] Values in cal mol^{-1} K^{-1}. Standard State = 1 bar and 298 K. Reference 3. [b] Values in cal mol^{-1} K^{-1}. Standard State = 1 atm (gas phase), 1 M (solution) and 298 K. [c] $\Delta S°[H^{\bullet}] = S°_f[H^{\bullet}]_g + \Delta S°_{solvation}[H^{\bullet}]$. Values in kcal mol^{-1} at 298 K. [d] Reference 4. [e] Reference 5. [f] Converted to 1 M standard state from unit mole fraction standard state. See Appendix 1 for derivation of this conversion.

Appendix 1:

$H^{\bullet}_{(g,\ 1\ atm)} \rightarrow H^{\bullet}_{(soln,\ unit\ mol\ fraction)}$ $\quad \Delta G°_{(solvation,\ H2)};\ T\Delta S°_{(solvation,\ H2)}$

$H^{\bullet}_{(soln,\ unit\ mol\ fraction)} \rightarrow H^{\bullet}_{(soln,\ 1\ M)}$ $\quad \Delta G°_{conversion};\ T\Delta S°_{conversion}$

$H^{\bullet}_{(g,\ 1\ atm)} \rightarrow H^{\bullet}_{(soln,\ 1\ M)}$ $\quad \Delta G°_{solvation}[H^{\bullet}];\ T\Delta S°_{solvation}[H^{\bullet}]$

In the equations above, $H^{\bullet}_{(a,\ b)}$ refers to $H^{\bullet}$ in phase *a* at standard state *b*. The mole fraction of gas, x_g, is related to the number of moles of gas n_g dissolved in the number of moles of liquid, n_{liq}, by eq A1.

$$x_g = \frac{n_g}{n_g + n_{liq}} \qquad \text{(A1)}$$

Rearranging:

$$n_g = \frac{x_g n_{liq}}{(1 - x_g)} \qquad \text{(A2)}$$

The concentration of dissolved gas, c_g, is defined as the number of moles per total volume, which is approximately the same as the volume of liquid for dilute solutions.

$$c_g = \frac{n_g}{V_{tot}} \approx \frac{n_g}{V_{liq}} \tag{A3}$$

Substituting n_g from eq A2 above, yields eq A4. V_m is the molar volume of the solvent liquid (= V_{liq} / n_{liq}).

$$c_g = \frac{\frac{x_g n_{liq}}{(1-x_g)}}{V_{liq}} = \frac{n_{liq} x_g}{V_{liq}(1-x_g)} = \frac{x_g}{V_m(1-x_g)} \tag{A4}$$

For H_2 in H_2O at 298 K.[5]

$x_{g(1\ atm)} = 1.411\times10^{-5}$

$$V_m(H_2O) = \frac{18.0153g}{mol} * \frac{mL}{0.9970480g} * \frac{L}{1000mL} = 0.018069\ L/mol$$

Therefore the concentration of dissolved gas at 1 atm is:

$$c_{g(1atm)} = \frac{x_g}{V_m(1+L)(1-x_g)} = \frac{1.411\times10^{-5}}{0.018069(1-1.411\times10^{-5})} = 7.809\times10^{-4}\ M \tag{A6}$$

Using proportionality we can determine what the concentration of dissolved gas $c_{g\ (x=1)}$ will be at x_g =1.

$$\frac{c_{g(1atm)}}{c_{g(x=1)}} = \frac{x_{g(1atm)}}{x_{g(x=1)}} \tag{A7}$$

$$c_{g(x=1)} = 7.809\times10^{-4}\ M \times \frac{1}{1.411\times10^{-5}} = 55.35M \tag{A8}$$

By definition using chemical potentials:

$$T\Delta S^{o}_{conversion} = \mu^{o}_{products} - \mu^{o}_{reactants} \tag{A9}$$

$$T\Delta S^{o}_{conversion} = \mu^{o}_{(soln,\ 1\ M)} - [\mu^{o}_{(soln,\ 1\ M)} + RT\ln[c_{g(x=1)}]] \tag{A10}$$

$$T\Delta S^{o}_{conversion} = -RT\ln[c_{g(x=1)}] \tag{A11}$$

$$T\Delta S^{o}_{conversion} = -RT\ln[55.35M] = -9.944\ kJ/mol = -2.377\ kcal/mol \tag{A12}$$

Using $\Delta S^{o}_{solvation}[H^{\bullet}]$ from reference 5 and eq A12 above:

$$T\Delta S^{o}_{solvation}[H^{\bullet}] = T\Delta S^{o}_{(solvation,\ H2)} + T\Delta S^{o}_{conversion} \tag{A13}$$

$$\Delta S^{o}_{solvation}[H^{\bullet}] = \Delta S^{o}_{(solvation,\ H2)} + (T\Delta S^{o}_{conversion})/T \tag{A14}$$

$$\Delta S^{o}_{solvation}[H^{\bullet}] = -25.478 - (2.377*1000)/298 = -17.50\ cal\ mol^{-1}\ K^{-1} \tag{A15}$$

(1) Matheson, I. B. C. *RSM-1000 Global Fit Software*, version 6.3.8; On-Line Instrument Systems (Olis), Inc. 1998.

(2) SPECFIT/32, versions v3.0.26 and v3.0.36; Spectrum Software Associates, 2000.

(3) NIST Standard Reference Database 69, June 2005 Release: NIST Chemistry WebBook. http://webbook.nist.gov/chemistry/

(4) Brunner, E. *J. Chem. Eng. Data* **1985**, *30*, 269-273.

(5) a) IUPAC, *Solubility Data Series*; Young, C. L. Ed.; Hydrogen and Deuterium, Vol. 5/6; Pergamon Press: New York, NY, 1981; 1-3, 259, 239. b) *Handbook of Chemistry and Physics, 87th ed.*; Lide, D.R. Ed.; CRC Press: Boca Raton, FL, 2006-2007, **6**-4.